C. R. Physique 3 (2002) 3–14

Électromagnétisme, optique/*Electromagnetism, optics*
(Solides, fluides : propriétés électroniques et optiques/*Solids, fluids: electronic and optical properties*)

DOSSIER

MICROCAVITÉS ET CRISTAUX PHOTONIQUES
MICROCAVITIES AND PHOTONIC CRYSTALS

Microcavity light emitting diodes as efficient planar light emitters for telecommunication applications

Daniel Ochoa [a], Romuald Houdré [a], Marc Ilegems [a], Christian Hanke [b], Bernt Borchert [b]

[a] Institut de micro et optoélectronique, École polytechnique fédérale de Lausanne, 1015 Lausanne, Switzerland

[b] Infineon Technologies CPR PH, Otto-Hahn-Ring 6, 81730 Munich, Germany

Received and accepted 23 November 2001

Note presented by Guy Laval.

Abstract Light emitting diodes (LEDs) can be coupled to optical fibers and used in telecommunication applications. Compared to laser diodes, the coupling is usually small, due to the isotropic emission of the source, combined with the large refractive index difference between the semiconductor and the outside medium. However, it is possible to greatly enhance the optical extraction of a planar LED by placing the source inside a microcavity which optical thickness is close to the wavelength of the emitted light. Some elementary design rules of a microcavity light emitting diode (MCLED) are explained here, and are illustrated on a real GaAs/$Al_xGa_{1-x}As$ device emitting at 880 nm. The surface external quantum efficiency of this MCLED reaches 14% into air and 20.6% with an encapsulation into an epoxy lens. These values are about 10 times larger than for a usual LED and are in good agreement with theoretical values, calculated with a plane waves model. To cite this article: D. Ochoa et al., C. R. Physique 3 (2002) 3–14. © 2002 Académie des sciences/Éditions scientifiques et médicales Elsevier SAS

light emitting diode / microcavity / brightness / Fabry–Pérot / semiconductors

La diode électroluminescente à microcavité : un émetteur de lumière planaire efficace pour des applications en télécommunications

Résumé Les diodes électroluminescentes (LEDs) peuvent être couplées à des fibres optiques et utilisées pour des applications en télécommunications. Ce couplage est généralement assez faible, en comparaison de celui qui est obtenu avec des diodes laser. Ceci est dû principalement à l'émission isotropique de la source, combinée à la grande différence d'indice de réfraction entre le semiconducteur et le milieu extérieur. Cependant, l'extraction optique d'une LED planaire peut être largement augmentée si la source est placée à l'intérieur d'une microcavité dont l'épaisseur est proche de la longueur d'onde de la lumière émise. Nous expliquons ici quelques règles fondamentales de conception d'une LED à microcavité (MCLED), et nous les illustrons avec l'exemple d'un composant réel en GaAs/$Al_xGa_{1-x}As$, émettant à 880 nm. Le rendement quantique externe de cette MCLED atteint 14% pour une emission dans l'air et 20,6% avec une encapsulation dans une lentille en époxy. Ces valeurs sont près de dix fois supérieures à celles d'une LED standard, et sont

E-mail address: daniel.ochoa@mines.org (D. Ochoa).

S1631-0705(02)01291-4/FLA

en bon accord avec les valeurs théoriques, calculées à l'aide d'un modèle d'ondes planes.
Pour citer cet article : D. Ochoa et al., C. R. Physique 3 (2002) 3–14.

diode électroluminescente / microcavité / brillance / Fabry–Pérot / semiconducteurs

1. Introduction

Light emitting diodes (LEDs) have many applications, in the visible range as well as in the infrared for telecommunications [1]. Concerning directionality, efficiency and modulation speed, laser diodes perform better than LEDs. However, LEDs are easier to make, cheaper and more reliable. Moreover, laser light coherence may have some disadvantages by giving speckle and security problems.

LEDs are mainly used as alphanumeric indicators, in remote controls and for short distance telecommunications. In the visible range, the number of applications has dramatically increased in the last decade, by the use of new quaternary compound materials such as $(Al_xGa_{1-x})_{0.5}In_{0.5}P$ and $Al_xIn_yGa_{1-x-y}N$, and by new growth techniques such as MBE and MOCVD. These new LEDs cover almost all the visible wavelength range and are much more efficient than the previous LED generations in GaP and $GaAs_xP_{1-x}$. First of all, they allow the fabrication of LED lamp bulbs that could one day replace incandescent bulbs [2,3]. The major advantages of LEDs are their very long lifetime: over 100 000 hours, and their low electrical consumption: about 30 times less than for incandescent bulbs, for the present technology. White light is achieved by placing together red, green and blue LEDs or by covering the epoxy dome of a blue LED with phosphor material. The second major application of LEDs in terms of market share concerns car back lights. Complementary stop lights, known as CHMSLs (center high mounted stop lights), are already found behind the rear window of cars. In the future, all stop and turn lights could be made of very bright red and amber LEDs [1,4]. One of the several advantages is the driver's security: the response of an LED is typically 0.1 µs, compared to 200–300 ms for an incandescent bulb. LEDs will also be used in traffic lights, as is already the case in some countries. When this will be widespread, economies in electrical consumption and maintenance will be huge. Other applications of red LEDs can be mentioned, like printers or plastic optical fiber (POF) telecommunications for local area networks (LANs) in the 100–400 Mbit/s range. Finally, perhaps the most advertising application of visible LEDs is the giant screen [1]. A pixel of such a screen is made of red, green and blue LEDs and can produce a large panel of colors. Giant LED screens are already found in stadiums during major sport events, or on building facades like the Nasdaq building.

The main quantity that characterizes the efficiency of an LED is the external quantum efficiency:

$$\eta_{\text{ext}} = \frac{P_{\text{op}}}{I\hbar\omega} \tag{1}$$

where P_{op} (W) is the optical power, I (A) is the electrical current injected into the device and $\hbar\omega$ (eV) is the emitted photon energy. For visible LEDs, the luminous performance is derived from the external quantum efficiency, by taking into account the wavelength sensitivity of the human eye. This luminous performance is shown in Fig. 1 for commercial LEDs versus year [1,5]. According to the famous 'Craford's law', it has been multiplied by a factor of approximately 10 every 10 years.

Until recently, the rapid increase in LED's efficiency was mainly due to material improvements. Now, modern growth techniques can achieve very high quality material deposition, giving active zones with almost 100% internal quantum efficiency, meaning that each electron-hole pair entering the active zone recombines radiatively by producing a photon. Then, the main limitation in efficiency comes from the optical extraction factor, that gives the probability for an internal photon to be extracted in the outside medium. During the last decade the Hewlett Packard laboratories have made remarkable advances in LED optical engineering: use of a thick transparent layer on top of the structure [6], then of a transparent substrate

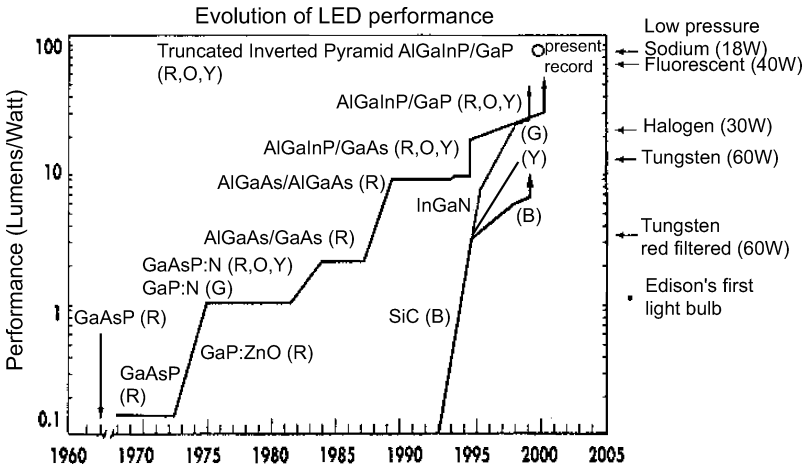

Figure 1. Evolution of the luminous performance of commercial visible LEDs. From reference [1].

[7,8], use of quantum wells (QWs) to minimize the optical absorption [9], and finally use of a truncated inverted pyramidal (TIC) shape achieving the present efficiency record of $\eta_{\text{ext}} = 55\%$ [10].

These efficiency improvements by geometrical modeling are very interesting for all the visible applications mentioned previously (except printers and LANs), where the LED's size is not an important issue. However, they do not apply for telecommunication applications, where coupling into an optical fiber is crucial. The core of a multimode fiber has typically a diameter of about 100 µm, much less than the size of usual parallelepipedic LEDs (about 400 µm), or even than TIC LEDs (more than 1 mm). For these 'tridimensional' LEDs, only the light emitted by the top surface could be coupled to a fiber. Increasing the coupling can only be done by adopting a planar geometry, where a maximum of light is emitted by the top surface, with a good vertical directionality.

Efficient planar LEDs are not easy to make [11]. The main difficulty comes from the large refractive index difference between the semiconductor (n_{in}) and the outside medium (n_{ext}). According to the Snell–Descartes law, light propagating inside the semiconductor can only be extracted if it fits within the cone defined by the critical angle of total internal reflection $\theta_{\text{c}} = \arcsin(n_{\text{ext}}/n_{\text{in}})$ with the normal of the interface. The rest of the light is totally internally reflected back into the semiconductor. For a GaAs LED $n_{\text{in}} = 3.6$ and the critical angle is about 16°. The surface optical extraction factor is simply given by a ratio of solid angles multiplied by the Fresnel transmission factor (note: for the optical extraction factor, we keep the same notation η_{ext} as for the external quantum efficiency of a LED. The two quantities are equal when the internal quantum efficiency is unity (forgetting the Purcell effect)):

$$\eta_{\text{ext}} \simeq \frac{2\pi(1-\cos\theta_{\text{c}})}{4\pi} T_{\text{Fresnel}} \simeq \frac{n_{\text{ext}}^2}{4n_{\text{in}}^2} T_{\text{Fresnel}} \tag{2}$$

giving 1.4% for an extraction into air, and 4% into epoxy. These figures are very low compared to laser diodes, that achieve over 50% external quantum efficiency, very high directionality and almost monochromatic emission. Therefore, in order to compete with laser diodes in the telecommunications market, large progresses in planar LEDs are expected.

One way to enhance the optical extraction of a planar LED is to place the active QWs inside a microcavity [12]. The objective is to modify the internal angular emission pattern, in order to force the light emission into the extraction cone (see Fig. 2). The basic bricks of a so-called 'microcavity LED' or MCLED are the following. First, the thickness of the microcavity is chosen to give a mode resonance, the 'cavity

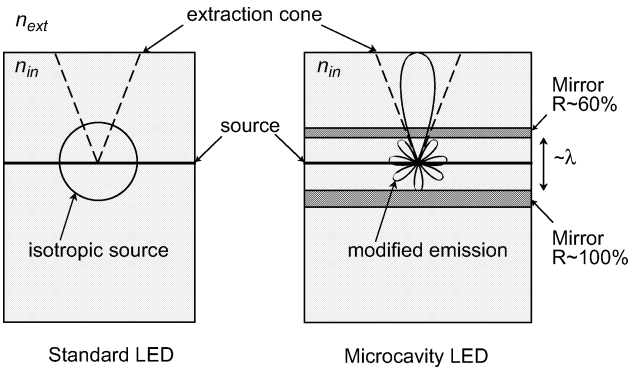

Figure 2. In a standard LED, light is emitted isotropically at the source. Because of the refractive index difference between the semiconductor and the outside medium, only the light emitted into the cone defined by the critical angle of total internal reflection can be extracted. Into air and for a GaAs LED, this represents 1.4% of the total source emission. In a Microcavity LED (MCLED), the source emission is modified by the optical confinement produced by two mirrors. A large fraction of light is emitted into a resonant mode which is almost entirely contained inside the extraction cone. This enhances significantly the surface extraction compared to a standard LED.

mode', in a direction close to the normal of the surface. This thickness must be small, in order to maximize the fraction of light going into the cavity mode. Secondly, the QWs are placed at an antinode position of the mode field, in order to maximize the mode emission. Finally, the back mirror is chosen to be more reflective than the front one and the mode emission is mainly directed towards the top surface, avoiding back emission. These basic elements will be detailed in the next section.

The study of MCLEDs started in the early 90s, with the works of Yokoyama [13,14], Björk, Yamamoto [15,16], Hunt and Schubert [17–21]. They showed, that a MCLED is brighter and spectrally purer than a classical LED. In 1997, Baets, DeNeve and Blondelle at the IMEC laboratory found that the extraction of a MCLED is enhanced when there is a negative detuning between the source emission wavelength and the resonance wavelength [22]. Moreover, they measured a better efficiency for their biggest diodes, suggesting some recycling effect in the active zone. With a 1.5 mm square LED, using back emission and a GaAs transparent substrate, they achieved the record external quantum efficiency of 20%. This value has to be compared to the 1.4% obtained with a classical LED. Some improvements were obtained by the group of N. Holonyak Jr. with GaAs/AlOx Bragg mirrors and a tunnel junction [23], reaching $\eta_{\text{ext}} = 27\%$. The first part of this article gives a short theoretical description of the MCLED, aimed at a basic understanding of the underlying physics. The second part gives an example of design, fabrication and characterization of a MCLED emitting by the surface at 880 nm [24].

2. Basic physics of the microcavity light emitting diode

Schematically, a MCLED is a Fabry–Pérot cavity surrounding a planar source. We first analyze this simple model, assuming a plane wave monochromatic emission and a very large finesse. Then, we introduce some angular broadening and some detuning between the source emission wavelength and the resonance wavelength. This ideal model is unfortunately too optimistic concerning the extraction efficiency, and some detrimental effects have to be taken into account: absorption, leaking losses, and the phase angular dependence of distributed Bragg reflectors (DBRs). Finally, we introduce a more accurate description of the MCLED, based on numerical calculations.

2.1. The Fabry–Pérot model

A basic representation of a MCLED is obtained by placing two mirrors on top and below a light source (see Fig. 3). For the sake of simplicity, we assume that the mirrors are ideal, with field reflectivities r_1 and

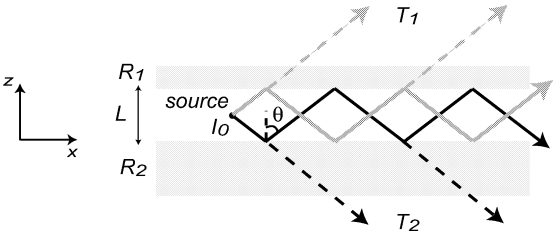

Figure 3. Basic representation of a MCLED, as a Fabry–Pérot with an internal point source.

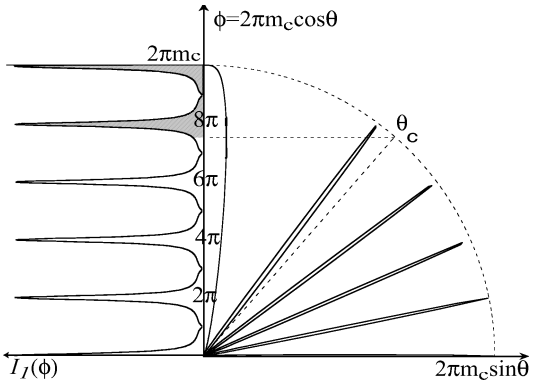

Figure 4. Right diagram: polar representation of the power emitted at the source of the MCLED. Left diagram: emitted power vs. round-trip dephasing ϕ. Light which is able to be extracted ($\theta < \theta_c$) corresponds to the shaded area. θ_c is the critical angle of total internal reflection between the semiconductor and the outside medium. The surface extraction factor of the MCLED is equal to the ratio between the shaded area and the total area of the curve.

r_2 real and positive. We note: $R_{1,2} = |r_{1,2}|^2$, $T_{1,2} = 1 - R_{1,2}$. The emitted light is made of monochromatic plane waves with wavelength λ_0 and intensity I_0, coming from a point source placed in the middle of the cavity. The distance between the two mirrors is noted L, the refractive index of the material is n_{in}.

The intensity of the transmitted field is given by [25,26]:

$$I_1(\phi) = I_0 \frac{T_1}{(1 - r_1 r_2)^2} \text{Ay}(\phi)\zeta(\phi) \tag{3}$$

$$\text{with:} \quad \phi(\theta) = n_{\text{in}} k_0 L \cos\theta = n_{\text{in}} \frac{2\pi}{\lambda_0} L \cos\theta \tag{4}$$

$$\text{Ay}(\phi) = \frac{1}{1 + C \sin^2 \phi}, \quad \text{with the constant } C = \frac{4 r_1 r_2}{(1 - r_1 r_2)^2} \tag{5}$$

$$\zeta(\phi) = 1 + R_2 + 2 r_2 \cos\phi \tag{6}$$

$\text{Ay}(\phi)$ is the Airy function and $\zeta(\phi)$ is known as the antinode factor.

We are interested in the fraction of light that is extracted into the outside medium (n_{out}). This transmitted power is represented in Fig. 4 [12] for the following assumptions:

(i) the reflectivity of the back mirror is maximal: $R_2 = 1$, so that all the light is directed towards the top surface;

(ii) the finesse of the cavity ($F = \pi\sqrt{r_1}/(1 - r_1)$) is very large, meaning that R_1 is close to unity;

(iii) the most vertical resonance of the Fabry–Pérot cavity occurs exactly at the normal direction $\theta = 0$, meaning that there is an integer m_c satisfying: $\phi(0) = n_{\text{in}} k_0 L = 2\pi m_c$. $m_c = n_{\text{in}} L/\lambda_0$ is called the 'order of the MCLED' (the quantity $m = 2m_c$ is usually called the 'order of the cavity').

With these assumptions, it can be shown [12] that the fraction of extracted light η_{ext} is given by the ratio between the shaded area (limited by the critical angle of total internal reflection θ_c), and the total area below the curve $I_1(\phi)$. Moreover all the peaks have exactly the same integral weight, and since the finesse of the cavity is very large, η_{ext} is simply given by the ratio between the number of modes present inside the extraction window, divided by the total number of modes m_c.

If m_c is large (a simple evaluation gives $m_c > 2n_{in}^2/n_{ext}^2$), this ratio tends toward the ratio of solid angles between the extraction window and the half space: $\eta_{ext} \to n_{ext}^2/(2n_{in}^2)$, which is exactly twice the optical surface extraction factor of a classical LED (see equation (2)), when forgetting the Fresnel transmission factor. The gain only comes from the incoherent reflection on the back mirror.

More interesting, if m_c is small enough, so that there is only one mode in the extraction window, one gets:

$$\eta_{ext} = \frac{1}{m_c} \tag{7}$$

giving potentially very large extraction values. In particular, if $m_c = 1$, what is usually referred as a 'λ-cavity', $\eta_{ext} = 100\%$: all the emitted light is extracted. Unfortunately, our model is so simplified that this is never the case for real MCLEDs. A more elaborate model has to include several detrimental effects, that will be detailed in Sections 2.2 and 2.3. First of all, we examine the effect of modal angular broadening, due to the finite cavity finesse.

2.2. Detuning

Here, unlike the hypothesis of the previous paragraph, the cavity finesse is not supposed to be very large, and the cavity mode is not exactly vertical. The quantity δ, called 'detuning', is defined so that:

$$n_{in}k_0L = 2\pi m_c\left(1 - \frac{\delta}{\lambda_0}\right) \tag{8}$$

giving:

$$\delta = \lambda_0 - \lambda_{FP} \tag{9}$$

where $\lambda_{FP} = Ln_{in}/m_c$ is the 'Fabry–Pérot wavelength' of the cavity. By definition, λ_{FP} is the wavelength of the source emission that gives a normal resonance of the cavity mode.

The optical extraction factor η_{ext} of a MCLED is very sensitive to the detuning, as can be seen in Fig. 5. Like in Fig. 4, η_{ext} is given by the ratio between the shaded areas below the vertical curves, divided by the total areas below these curves. It appears clearly that the extraction is larger when the detuning is negative, and lower when it is positive. It can be shown [12,27] that η_{ext} is maximum when the Airy peak of the cavity mode is placed symmetrically in the phase extraction window $[\phi(\theta_c), \phi(0)]$, giving:

$$\delta = -\frac{n_{ext}^2}{4n_{in}^2}\lambda_0 \tag{10}$$

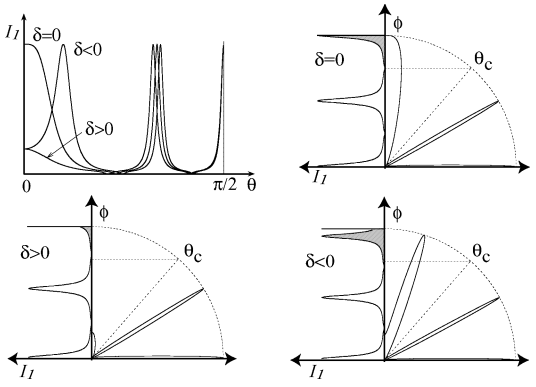

Figure 5. Top left: intensity I_1 transmitted through the top mirror of a MCLED vs. emission angle θ (inside the semiconductor) and for different detunings δ. Other graphs: representations of I_1 on polar diagrams for $\delta = 0$, $\delta > 0$, and $\delta < 0$. Shaded areas correspond to extracted light.

and a 'rabbit ear' shape of the emission into the outside medium, with a maximum of the lobes at 45° from the normal of the surface. However, when fiber coupling is required, the optimum of equation (10) is not valid any more, since the emission directionality becomes crucial. A trade off between directionality and total extraction efficiency has to be found.

2.3. Additional effects

The introduction of some mode angular broadening and of a detuning between the source emission and the resonance wavelength is a main improvement of the basic Fabry–Pérot model of Section 2.1. There are other effects that must be taken into account in order to improve this model [12,28]. Unfortunately, almost all of them are detrimental to the extraction.

2.3.1. *Absorption into the active zone*

When traveling into the microcavity, light is partly absorbed into the active zone. The loss of each pass is usually less than 1%, and the total loss of the cavity mode remains reasonable: for a top mirror reflectivity of 60%, about 93% of the light emitted into the cavity mode has left the structure after 5 round trips into the cavity. Light going into the guided mode (see Section 2.4) is more subject to this absorption, leading to the recycling effect: photons from the high-energy part of the emission spectrum can be absorbed into the active zone by creating electron-hole pairs that, in turn, can recombine radiatively and emit photons. This effect on the external quantum efficiency is proportional to $(1 - \eta_{\text{int}}\eta_{\text{abs}})^{-1}$ [29], where η_{int} is the internal quantum efficiency of the active zone, and η_{abs} is the fraction of reabsorbed light. It appears that the efficiency increase is only important for high quality active zones, when η_{int} is close to unity.

2.3.2. *Leaking through the back mirror*

The reflectivity of the back mirror is never 100%, leading to losses. First of all, direct losses can be experienced by the cavity mode. For example, a back mirror of reflectivity $R_2 = 99\%$ leads to a net loss of 1% per pass, for each light round-trip inside the microcavity. Secondly, dielectric mirrors like DBRs are highly reflective only in a somewhat small (depending on the refractive index difference) angular region centered on the normal direction and known as the 'stopband'. DBRs play their role as good reflectors for the cavity mode, but act very badly for the other resonances: the reflectivity of a GaAs/AlAs DBR oscillates between 0 and 20% for all angles in the 20°–60° range. Light that escapes from the microcavity at these angles is known as 'leaky modes'. Although leaky modes are not detrimental to the cavity mode resonance, they represent a loss in terms of reabsorption into the active zone, and thus in terms of recycling. In a MCLED, they account for up to 50% of the total of emitted light. Their suppression therefore represents a major challenge.

2.3.3. *Spectral broadening*

Previous calculations were made for a monochromatic emission. This is never the case in a MCLED, and the spectral broadening of injected QWs is usually larger than 20 nm. This spectral broadening is always detrimental to extraction [27,28]. Moreover, it leads to a directionality loss, a spectral sharpening at each angular direction, and an angular separation of the wavelengths. This last point appears on the following equation:

$$\lambda_{\text{max}} \simeq \lambda_{\text{FP}} \sqrt{1 - \frac{n_{\text{ext}}^2}{n_{\text{in}}^2} \sin^2 \theta_{\text{ext}}} \tag{11}$$

where λ_{max} is the maximum of the spectral emission peak and θ_{ext} the external angle. There is a spectral blue-shift when θ_{ext} increases away from the normal direction.

2.3.4. *Non-ideal mirrors*

Our basic Fabry–Pérot model uses ideal mirrors, whose reflection dephasing is always zero. In practice, MCLEDs use metallic or DBR mirrors and this property is not valid. Angular variations of the dephasing can be important, resulting in efficiency losses. For example, with a DBR, the expression (7) of the extraction efficiency is replaced by:

$$\eta_{\text{ext}} = \frac{1}{m_{\text{c}} + m^{\theta}_{\text{DBR}}} \tag{12}$$

where the introduction of the effective order $m^{\theta}_{\text{DBR}} = n_{\text{in}} L^{\theta}_{\text{DBR}}/\lambda_{\text{FP}}$ can be interpreted as an increase of the cavity thickness by an 'angular penetration length' L^{θ}_{DBR}. L^{θ}_{DBR} has clearly to be distinguished from the usual wavelength penetration length L^{λ}_{DBR}, since L^{θ}_{DBR} becomes much larger than L^{λ}_{DBR} when the refractive index difference of the DBR increases [28,30].

2.4. Realistic MCLED

The basic Fabry–Pérot model, and its additional effects listed in the previous section, give an introduction to the physics involved in a MCLED. However, in order to design a real device, this model is limited. Several effects like detuning, spectral broadening, absorption, and DBR dephasing, have to be evaluated accurately and simultaneously. Moreover, the active zone is not a simple point source, giving a complex emission pattern with both TE and TM components. The total emitted power is not even constant and depends on the optical confinement. This effect, known as the 'Purcell effect' [31], is really important for 3D confinements only, but can reach a 10% increase in the planar confinement of a MCLED. In practice the design of a MCLED can only be done numerically.

We use a spontaneous emission model [26] based on the decomposition of the source emission into plane waves, and on the transfer matrix method, as suggested by W. Lukosz [32]. This model is valid for any dielectric multilayered structure, and takes into account the absorption in each layer, the QW source emission with its spectral and angular dependences, both TE and TM polarizations, and the Purcell effect. The direct output of the numerical code is the normalized power emitted at the source and both into the outside medium and into the substrate.

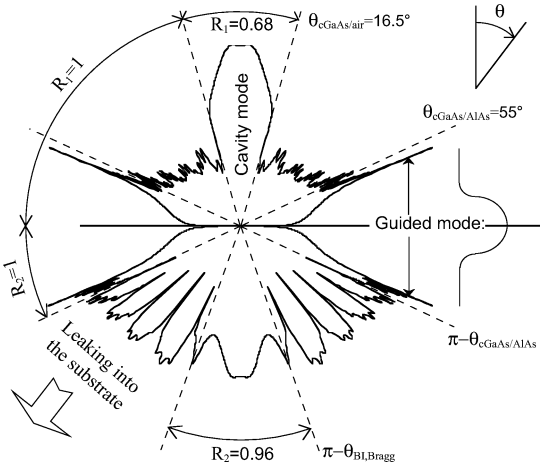

Figure 6. Calculation of the internal power emitted at the source of a typical GaAs/AlAs MCLED formed by two Bragg mirrors.

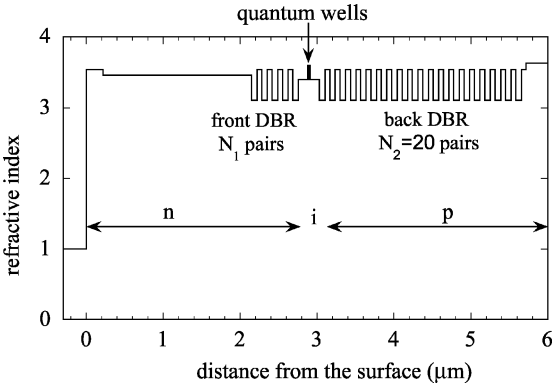

Figure 7. Refractive index profile of the MCLED described in this paper.

The Fig. 6 shows an example of calculation, for a typical MCLED formed by two GaAs/AlAs DBRs (3 pairs front and 20 pairs back), a λ-cavity in GaAs and a zero detuning. The power emitted at the source is represented in polar and logarithmic scale, for the TE polarization. The cavity mode appears inside the extraction window. It is mainly directed towards the surface because of the larger reflectivity of the back mirror ($R_2 = 96\%$) compared to the front one ($R_1 = 68\%$). As explained earlier, the low reflectivity of the back DBR outside the stopband leads to leaky modes. Leaky modes represent a large fraction of light escaping into the substrate. They do not appear for top emission, because of the total internal reflection at the GaAs/air interface, which starts inside the stopband of the front DBR. For an angular propagation close to $\theta = 90°$, light faces total internal reflection at the GaAs/AlAs interface. It remains confined in the cavity and travels laterally through the structure as a guided mode.

Our simulation model takes into account the lateral propagation of the guided mode and gives access to the lateral extraction factor, the amount of light absorbed in the QWs [29], and therefore the recycling factor.

3. Example of design fabrication and characterization of a real MCLED

In order to illustrate the previous theoretical concepts, we present here some calculations and measurements made on a typical MCLED.

3.1. Optical design

The heterostructure of the device is shown in Fig. 7 [24]. It has two $In_{0.06}Ga_{0.94}As$ QWs emitting at 880 nm and placed in the middle of an $Al_{0.3}Ga_{0.7}As$ λ-cavity. Optical confinement is provided by two $Al_{0.1}Ga_{0.9}As/Al_{0.8}Ga_{0.2}As$ DBRs. The back DBR has 20 pairs, and the front one a number N_1 of pairs that has to be optimized. The GaAs substrate and the back DBR are p-doped, the cavity is undoped, and the front DBR is n-doped. For a better electronic lateral diffusion, a thick (2 µm) n-doped $Al_{0.2}Ga_{0.8}As$ layer is placed between the surface and the front DBR. It provides homogeneous injection conditions for a large range of current densities, and reduces the top n-contact shadowing.

The optical design of the MCLED is made by maximizing the external quantum efficiency η_{ext} for different values of N_1 and λ_{FP} (λ_{FP} is directly related to the thickness of the cavity L). The optimum is found for $\lambda_{FP} = 920$ nm ($L = 271$ nm) and $N_1 = 4$ pairs, giving a maximum monochromatic external quantum efficiency of 23.9%. The calculation assumptions are the following:

(i) the internal quantum efficiency is unity: $\eta_{int} = 1$;
(ii) light recycling into the QWs is not taken into account;
(iii) the external medium has a refractive index of 1.5, like epoxy;
(iv) DBRs are phase matched with the cavity: $\lambda_{DBR} = \lambda_{FP} = Ln$, where λ_{DBR} is the central wavelength of the DBRs and $n = 3.4$ (at 880 nm), is the refractive index of the cavity medium;
(v) $Al_xGa_{1-x}As$ refractive indexes are taken from reference [33];
(vi) absorption into the QWs is fixed at 0.3% per QW and per pass (3000 cm^{-1} for 10 nm thick QWs);
(vii) free carrier absorption due to doping is set to $\alpha_{dop} = 10$ cm^{-1} for all layers [34,35].

3.2. Fabrication and measurements

The device is fabricated with a three steps processing. Small circular n-contacts (Ni–Ge–Au–Ni–Au) are first deposited on the n-doped surface. The structure is then wet-etched, forming large circular mesas centered on the n-contact and going deep through the structure, beyond the back DBR. The final processing step is a Ti–Pt–Au metalization of the p-doped surface (substrate) at the feet of the mesas. A schematic section of the device is shown on Fig. 8a.

The wafer is cleaved into 500 µm × 500 µm square pieces containing one MCLED each. These pieces are sticked on a TO header with some conducting epoxy, acting as a p-contact with the substrate. The top

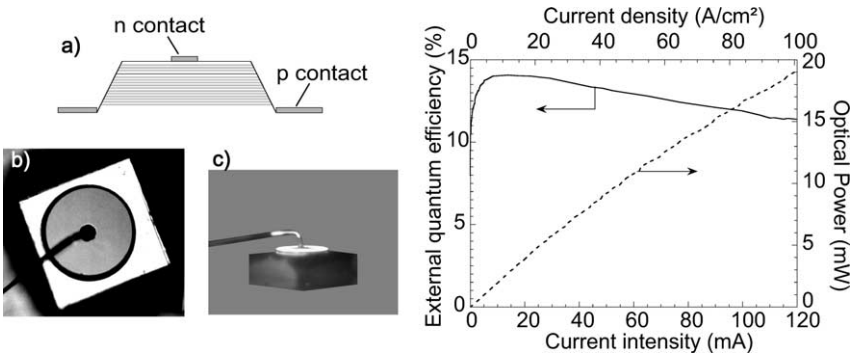

Figure 8. Left part: (a) Schematic section of the MCLED device; (b) MCLED device cleaved and contacted by wire-bonding; (c) same device under electrical injection. Right part: total external quantum efficiency of the MCLED, placed into an integration sphere. The current is pulsed with a duty cycle of 10%.

n-contact is wire-bonded, as shown on Fig. 8b. The diameter of the bond is 80 µm and the top diameter of the mesa about 370 µm. The contact shadowing is therefore equal to $(80/370)^2 = 4.7\%$.

The TO header is inserted into a calibrated integration sphere, measuring the total optical power emitted by the MCLED. The external quantum efficiency η_{ext} is obtained by dividing the optical power by the current intensity and by the photon energy (1.5 eV). The result is shown on the Fig. 8, for a pulsed injection current with a duty cycle of 10%. η_{ext} reaches the maximum value of 14% for a current injection of about 10 mA.

The final fabrication step is to encapsulate the device into an epoxy dome. Instead of the usual spherical dome, we use a lens-type shape [24]. The external quantum efficiency is still measured with the integration sphere and reaches a maximum value of 20.6% for a current of 10 mA.

3.3. Measurements analysis

A complete analysis of various measurements performed on the MCLED (reflectivity, I–V, emission spectrum, angular emission pattern, external quantum efficiency, angular resolved spectra) can be found in references [24,28]. We give here only a short analysis of the external quantum efficiency measurements. The calculations give:

$$\begin{aligned} &\text{air:} \quad \eta_{\text{surf}} = 13.6\%, \quad \eta_{\text{lat}} = 1.5\% \\ &\text{epoxy:} \quad \eta_{\text{surf}} = 19.2\%, \quad \eta_{\text{lat}} = 2.4\% \end{aligned} \tag{13}$$

where η_{surf} and η_{lat} are the surface and lateral external quantum efficiencies [29]. The fraction of light which is reabsorbed into the QWs is $\eta_{\text{abs}} = 15.3\%$ for an extraction into air and 13.8% into epoxy. By taking into account the recycling effect and the shadowing due to the top contact $\tau_{\text{shad}} = 4.7\%$, the total external quantum efficiency of the MCLED is given by:

$$\eta_{\text{ext}} \simeq \frac{\eta_{\text{int}}(\eta_{\text{surf}}(1 - \tau_{\text{shad}}) + \eta_{\text{lat}})}{1 - \eta_{\text{int}}\eta_{\text{abs}}} \tag{14}$$

The internal quantum efficiency η_{int} is finally found by fitting η_{int} in order to match η_{ext} with the measured values of 14% into air and 20.6% into epoxy. For $\eta_{\text{int}} = 85\%$, the calculation gives $\eta_{\text{ext}} = 14.2\%$ into air and 20% into epoxy, which is reasonably close to the measured values.

4. Conclusion

On the contrary to usual LEDs, the source emission of a MCLED is not isotropic. It is confined between two planar mirrors and forms optical resonant modes. The most vertical mode is extracted through the top mirror because it fits into the extraction cone of total internal reflection. If the optical thickness of the cavity is close to the wavelength of the emitted light, the surface external quantum efficiency of the MCLED can be much larger than for a usual LED.

The basic physics of the MCLED was described in the first part of this article. Some design rules were given, as well as additional effects that are important regarding the extraction efficiency. In the second part, a practical example of MCLED is analyzed. The device is in GaAs/$Al_xGa_{1-x}As$ and is 880 nm surface emitting. The measures are in good agreement with the theory. They give an external quantum efficiency of 14% into air and 20.6% with an encapsulation into a lens-shape epoxy dome. The brightness achieved by this MCLED is therefore much larger than with a usual LED.

References

[1] M.G. Craford, G.B. Stringfellow, High brightness light emitting diodes, in: M.G. Craford, G.B. Stringfellow (Eds.), Semiconductors and Semimetals, Vol. 48, Academic Press, San Diego, 1997.

[2] R. Dixon, Engineering with high brightness LEDs, Compound Semicond. 6 (2) (2000) 40–45.

[3] R. Haitz, F. Kish, J. Tsao, J. Nelson, Another semiconductor revolution: this time it's lighting, Compound Semicond. 6 (2) (2000) 34–37.

[4] F.A. Kish, D.C. Defevere, D.A. Vanderwater, G.R. Trott, R.J. Weiss, J.S. Major, High luminous flux semiconductor wafer-bonded AlGaInP/GaP large-area emitter, Electron. Lett. 30 (21) (1994) 1790–1791.

[5] M. Meyer, 'Craford's law' and the evolution of the LED industry, Compound Semicond. 6 (2) (2000) 26–30.

[6] K.H. Huang, J.G. Yu, C.P. Kuo, R.M. Fletcher, T.D. Osentowski, L.J. Stinson, A.S.H. Liao, Twofold efficiency improvement in high performance AlGaInP light-emitting diodes in the 555–620 nm spectral region using a thick GaP window layer, Appl. Phys. Lett. 61 (9) (1992) 1045–1047.

[7] F.A. Kish, F.M. Steranka, D.C. DeFevere, D.A. Vanderwater, K.G. Park, C.P. Kuo, T.D. Osentowski, M.J. Peanasky, J.G. Yu, R.M. Fletcher, D.A. Steigerwald, M.G. Craford, V.M. Robbins, Very high-efficiency semiconductor wafer-bonded transparent substrate $(Al_xGa_{1-x})_{0.5}In_{0.5}P$/GaP light-emitting diodes, Appl. Phys. Lett. 64 (21) (1994) 2839–2841.

[8] F.A. Kish, D.A. Vanderwater, D.C. DeFevere, D.A. Steigerwald, G.E. Hofler, K.G. Park, F.M. Steranka, Electron. Lett. 32 (1996) 132.

[9] N.F. Gardner, H.C. Chui, E.I. Chen, M.R. Krames, J.W. Huang, F.A. Kish, S.A. Stockman, 1.4 × efficiency improvement in transparent-substrate $(Al_xGa_{1-x})_{0.5}In_{0.5}P$ light-emitting diodes with thin ($\leqslant$ 2000 A) active regions, Appl. Phys. Lett. 74 (15) (1999) 2230–2232.

[10] M.R. Krames, M. Ochiai-Holcomb, G.E. Holfer, C. Carter-Coman, E.I. Chen, I.H. Tan, P. Grillot, N.F. Gardner, H.C. Chui, J.W. Huang, S.A. Stockman, F.A. Kish, M.G. Craford, S.T. Tan, C.P. Kocot, M. Hueschen, J. Posselt, B. Loh, G. Sasser, D. Collins, High-power truncated-inverted-pyramid $(Al_xGa_{1-x})_{0.5}In_{0.5}P$/GaP light-emitting diodes exhibiting $\geqslant$ 50% external quantum efficiency, Appl. Phys. Lett. 75 (16) (1999) 2365–2367.

[11] W.N. Carr, Photometric figures of merit for semiconductor luminescent sources operating in spontaneous mode, Infrared Phys. 6 (1966) 1–19.

[12] H. Benisty, H.D. Neve, C. Weisbuch, Impact of planar microcavity effects on light extraction: I. Basic concepts and analytical trends, IEEE J. Quantum Electron. 34 (1998) 1612.

[13] H. Yokoyama, K. Nishi, T. Anan, H. Yamada, S.D. Brorson, E.P. Ippen, Enhanced spontaneous emission from GaAs quantum wells in monolithic microcavities, Appl. Phys. Lett. 57 (26) (1990) 2814–2816.

[14] H. Yokoyama, Physics and device applications of optical microcavities, Science 256 (1992) 66–70.

[15] G. Björk, S. Machida, Y. Yamamoto, K. Igeta, Modification of spontaneous emission rate in planar dielectric microcavity structures, Phys. Rev. A 44 (1991) 669–681.

[16] G. Björk, H. Heitmann, Y. Yamamoto, Spontaneous-emission coupling factor and mode characteristics of planar dielectric microcavity lasers, Phys. Rev. A 47 (5) (1993) 4451–4463.

[17] E.F. Schubert, Y.H. Wang, A.Y. Cho, L.W. Tu, G.J. Zydzik, Resonant cavity light-emitting diode, Appl. Phys. Lett. 60 (8) (1992) 921–923.

[18] N.E.J. Hunt, E.F. Schubert, D.L. Sivco, A.Y. Cho, G.J. Zydzik, Power and efficiency limits in single-mirror light emitting diodes with enhanced intensity, Electron. Lett. 28 (23) (1992) 2169–2171.

[19] N.E.J. Hunt, E.F. Schubert, R.A. Logan, G.J. Zydzik, Enhanced spectral power density and reduced linewidth at 1.3 μm in an InGaAsP quantum well resonant-cavity light-emitting diode, Appl. Phys. Lett. 61 (19) (1992) 2287–2289.
[20] E.F. Schubert, N.E.J. Hunt, M. Micovic, R.J. Malik, D.L. Sivco, A.Y. Cho, G.J. Zydzik, Highly efficient light-emitting diodes with microcavities, Science 265 (1994) 943–945.
[21] N.E.J. Hunt, High efficiency, narrow spectrum resonant cavity Light Emitting Diodes, in: E. Burstein, C. Weisbuch (Eds.), Confined Electrons and Photons, Plenum Press, New York, 1995, pp. 703–714.
[22] H. De Neve, J. Blondelle, P.V. Daele, P. Demeester, R. Baets, Recycling of guided mode light emission in planar microcavity light emitting diodes, Appl. Phys. Lett. 70 (1997) 799–801.
[23] J.J. Wiener, D.A. Kellog, N. Holonyak, Tunnel contact junction native-oxide aperture and mirror vertical-cavity surface-emitting lasers and resonant-cavity light-emitting diodes, Appl. Phys. Lett. 74 (1999) 926–928.
[24] D. Ochoa, R. Houdré, R.P. Stanley, M. Ilegems, C. Hanke, B. Borchert, 880 nm surface emitting microcavity light emitting diode, in: H.W. Yao, E.F. Schubert (Eds.), Light-Emitting Diodes: Research, Manufacturing, and Applications V, Proceedings of SPIE, Vol. 4278, 2001, pp. 70–80.
[25] A. Kastler, Atomes à l'intérieur d'un interféromètre Pérot–Fabry, Appl. Opt. 1 (1) (1962) 17–24.
[26] R.P. Stanley, H. Benisty, M. Mayer, Method of source terms for dipole emission modification in modes of arbitrary planar structures, J. Opt. Soc. Am. A 15 (1998) 1192–1201.
[27] D. Ochoa, R. Houdré, R.P. Stanley, U. Oesterle, M. Ilegems, Device simultaneous determination of the source and cavity parameters of a microcavity light-emitting diode, J. Appl. Phys. 85 (1999) 2994–2996.
[28] D. Ochoa, Diodes électroluminescentes planaires à haut rendement d'extraction lumineux, PhD thesis, École polytechnique fédérale de Lausanne, Micro and Opto-electronics Institute, EPFL, 1015 Lausanne, Switzerland, 2001.
[29] D. Ochoa, R. Houdré, R.P. Stanley, M. Ilegems, H. Benisty, C. Hanke, B. Borchert, Spontaneous emission model of lateral light extraction from heterostructure light-emitting diodes, Appl. Phys. Lett. 76 (22) (2000) 3179–3181.
[30] R. Stanley, R. Houdré, M. Ilegems, Limits of high contrast mirrors for microcavity LEDs, in preparation.
[31] E.M. Purcell, Phys. Rev. 69 (1946) 681.
[32] W. Lukosz, Light emitted by multipole sources in thin layers. I. Radiation patterns of electric and magnetic dipoles, J. Opt. Soc. Am. 71 (1981) 744–754.
[33] S. Adachi, Optical properties of AlGaAs: Transparent and interband transition regions (tables), in: S. Adachi (Ed.), Properties of Aluminium Gallium Arsenide, Vol. 7, Inspec Publication, 1991, pp. 126–140.
[34] K.J. Ebeling (Ed.), Integrated Opto-Electronics, Springer-Verlag, New York, 1991.
[35] C. Dill, Fabrication and characterization of high efficiency microcavity light emitting diodes, PhD thesis, École polytechnique fédérale de Lausanne, DP IMO EPFL, 1015 Lausanne, CH, 1999.